CELLULAR & MOLECULAR BIOLOGY LETTERS
Volume 8, (2003) pp 1017 – 1033
http://www.cmbl.org.pl

Received 23 June 2003
Accepted 17 October 2003

FORCE GENERATION BY CELLULAR MOTORS

FRIEDRICH WANKA* and EVERARDUS J.J. VAN ZOELEN
Department of Cell Biology, University of Nijmegen, Toernooiveld 1
6525 ED Nijmegen, The Netherlands

Abstract: Cell motility processes in non-muscle cells depend on the activity of motor proteins that bind to either microtubules or actin filaments. From presently available data it must be concluded that the driving force is generated by transient interaction of the respective motors with microtubules or actin filaments which then activates the binding and hydrolysis of ATP. This reaction results in an abrupt discharge of the motor molecule, the direction of which is determined by the spatial orientation of its binding to the helical and polar vehicle. The latter is thereby propelled in its length direction and simultaneously undergoes an axial rotation, while the expelled motor exerts an oppositely directed current in the surrounding fluid, comparable to jet propulsion. Force production, propulsion velocities and energy requirements known from *in vitro* studies comply with those derived from the theory. The theory opens new ways for the understanding of cellular activities such as particle transport, mitosis and morphodynamics.

Key Words: Force Generation, myosin, kinesin, Actin Filament Propulsion, Plasma Streaming

INTRODUCTION

Active motility in living organisms, such as muscle contraction, mitotic chromosome segregation, as well as cell movement by flagella or cilia, and amoeboidal behaviour requires force generating processes at both the cellular and subcellular level. Many of these processes have been found to depend on the activity of evolutionary highly conserved motor proteins, based on interaction with either microtubules or actin filaments. Under suitable *in vitro* conditions all motors cause propulsion of their respective vehicles, powered by hydrolysis of nucleoside triphosphates, usually ATP. It seems therefore reasonable to assume that basically similar mechanisms of force generation underlie these various motility phenomena.

* Corresponding author

A generally accepted model for explaining muscle contraction is the sliding-filament hypothesis of Huxley [1], according to which filaments move past each other by the tilting of transient interfilament cross-bridges formed by myosin heads. The swinging cross-bridge model is appealing because of its apparent simplicity. This may be the reason why modified versions of this model have been suggested in attempts to explain other motion processes as well. Originally, the cross-bridge model was aimed to explain the sliding of actin and myosin filaments relative to each other. Its basic features are the binding of a myosin head that extends from the myosin filament to a specific site of the actin filament, whereupon it undergoes an ATP-powered tilting which moves one filament along the other over a discrete distance, usually assumed to amount to 10 nm. *In vitro* movements of actin filaments and microtubules are believed to occur via a similar transient cross-bridge formation with motors attached to a solid surface. However efforts to provide evidence for a predictable, discrete 10 nm (or 40 nm) step have failed (e.g. 2). Moreover light microscopic observations show simultaneously moving microtubules at different focal levels, indicating that most of them, if not all are propelled in suspension [3,4]. Data that conflict with the cross-bridge model in muscle have been discussed by Pollack [5].

We now present a general concept that involves force generation by a jet propulsion-like mechanism, which is compatible with the mentioned data and many others that have not been rationally explained in the past. It has been derived by a comparative analysis of experimental results on the kinetics of motor-vehicle and motor-nucleotide interactions in combination with structural data, in particular those obtained by crystallographic studies on relevant motor-nucleotide complexes. Briefly, the following steps are involved. Motor proteins bind to their respective vehicle in an orientation-specific manner, whereby the intramolecular rearrangement induced by the binding reaction results in an activation of the catalytic center. The resulting ATP hydrolysis then powers a stroke-like movement and immediate release of the motor molecule from the vehicle. Accordingly, the latter experiences a momentum of propulsion into one direction, while the expelled motor provokes an oppositely directed microcurrent in the surrounding fluid. The microcurrents produced along individual actin filaments or microtubules by such motor activities combine into plasma currents, the strength of which must be equivalent to the propulsive force exerted onto the respective vehicle.

EVIDENCE FOR A JET PROPULSION-LIKE FORCE GENERATION MECHANISM

In vivo plasma streaming and vehicle transport have been documented. For example, plasma streaming has been found to occur along bundles of actin filaments in the long internodial cells of characeae [6], while movements of individual microtubules have been observed in neuronal growth cones [7], but observations that would explain the molecular background of such a behaviour

are limited. On the other hand, *in vitro* studies on the propulsion of microtubules and actin filaments [e.g. 2,8] have revealed many significant data for a critical examination of the physical background of the proposed concept. Here we show that a jet propulsion-like mechanism can be inferred from known data on the kinetics and structural rearrangements induced in the motor proteins during motor-vehicle and motor-nucleotide interactions. One particular feature of the proposed mechanism is that the vehicle movement is counteracted by the drag exerted by the oppositely directed plasma flow. We further point out that in vitro observed vehicle propulsion velocities are compatible with measured force production and energy consumption.

Motor-vehicle and motor-nucleotide interactions

The architecture of the various myosins, kinesins and dyneins discovered so far may reflect to some extent the specific roles they fulfill in cellular activities. A property they all share is the ability to propel either actin filaments or microtubules in their longitudinal direction under suitable *in vitro* conditions [3,4,8-10]. A common minimum requirement for this activity is the possession of at least one, more or less pear-shaped, head domain that contains a catalytic center for ATP hydrolysis and a well-defined site for stereospecific binding to the respective vehicle [11-15]. Moreover, studies on molecular structures have revealed a great similarity between motor domains of kinesin and myosin [16]. Because of these and many other analogies discussed below, we make the operational assumption that the propulsive force is generated by largely homologous mechanisms in all motors.

Significant data on the steps of force production have been gathered by studies on the kinetics of motor-vehicle and motor-nucleotide interactions: 1) Motor molecules bind to their respective vehicles in a stereospecific orientation that is determined by the polarity of the vehicle. In the absence of nucleoside triphosphates the density of kinesin binding at saturating concentration reaches up to one motor molecule per tubulin heterodimer [17,18]. A binding density of the same order of magnitude can be inferred for myosin-actin filament interactions from electron micrographs [19] and from the finding that the stereospecific binding of one myosin head involves two consecutive actin monomers [14,15]. 2) All motor proteins are released from the vehicles by ATP but not by its nonhydrolyzable homologues. Significantly, GTP, which can replace ATP as energy generator in kinesin motor activity, also causes the dissociation of this motor from microtubules [3,20]. 3) The ATPases of all motor proteins are activated by interaction with their specific vehicles [2,3,17,21,22]. A burst of ATPase activity is observed when kinesin is released from preformed microtubule-kinesin complexes upon addition of excessive ATP concentrations.

These findings can be summarized by a sequence of biochemical reactions describing the stepwise interactions of the vehicle (V), motor protein (M) and ATP, as shown in Fig. 1. In the absence of ATP, step 1 must result in an accumulation of VM, which explains the excessive binding of the motors to the

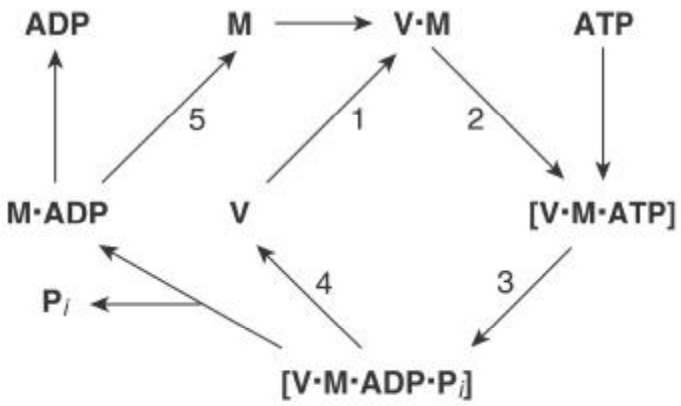

Fig. 1. Sequence of motor-vehicle and motor-nucleotide interactions during the force generating cycle. V, vehicle; M, motor. For details see text.

respective vehicles observed under suitable *in vitro* conditions. The stability of such complexes in the presence of nonhydrolyzable ATP homologues suggests that hydrolysis of the nucleotide is essential for the motor-vehicle dissociation. This is corroborated by the finding that inhibition of the ATPase by N-ethylmaleimide leads to an increase of microtubule-bound kinesin [23]. The intermediate states in brackets are not detectable by presently available techniques owing to their short half-lifes. At saturating ATP concentrations the flow through the cycle is limited by the low rate of ADP release from the various motors (step 5) [24-27]. Accordingly, stabilization of the motor-ADP complex by binding of vanadate or other P_i homologues to the γ-phosphate position of the ATP binding site inhibits both the ATPase and motor activity [28,29]. Studies with myosin II subfragment 1 indicate that this might be due to the inability of proper stereospecific interaction of the myosin-ADP intermediate with the actin filament [14,15,30,31] thereby preventing the completion of the catalytic cycle. This makes the ADP release to the limiting step in the myosin turnover during the catalytic process at cellular ATP levels. A similar effect on motor-microtubule interaction by ADP is indicated by the finding that binding constants in the motor-ADP state are significantly lower than in the nucleotide-free state: 3000-fold for kinesin and 50-fold for the ncd motor [32]. The existence of a free dynein-ADP intermediate is corroborated by the finding that the rate of ATP hydrolysis, which increases four to six fold in the presence of microtubules, is enhanced another 30-fold if the motor is chemically linked to them [33-35]. The latter must be ascribed to the increased probability to achieve the proper stereospecific interaction between the two complementary binding faces owing to their close proximity at the time when the ADP is released from the catalytic site.

Structural rearrangements of motor molecules

The various steps of the kinetic sequence can be assigned to specific conformational rearrangements of the motor molecules, as shown in Fig. 2.

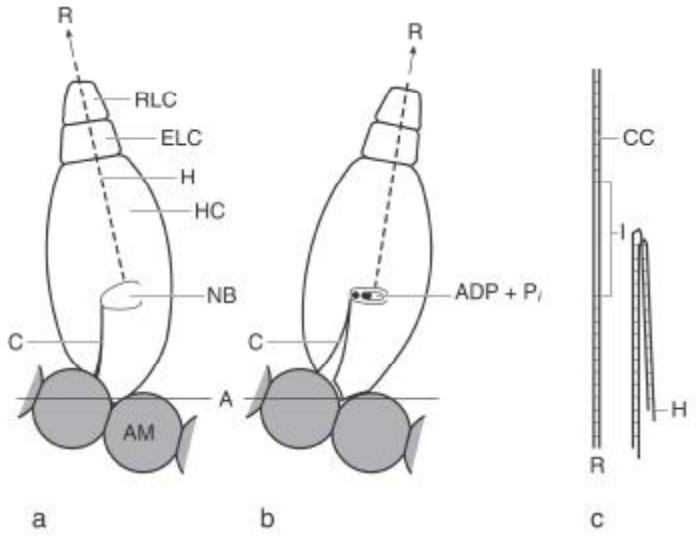

Fig. 2. Diagram of the molecular rearrangement in myosin II during force generation. a) The nucleotide-free myosin head binds to two consecutive monomers (AM) of an actin filament with the cleft (C) at the binding face closed. b) The molecular rearrangement caused by ATP binding and hydrolysis results in an opening of the cleft which exerts a rotational momentum onto the myosin head and concomitantly disrupts the myosin-actin interaction. The COOH-terminal α-helical domain (H) of the myosin heavy chain is simultaneously retracted into the head. c) Left: Rod domain (R) of a myosin II type motor. The α-helices of the rod-stabilizing coiled coil (cc and cross-bars) are drawn as straight lines for simplicity. Right: A sharp bent occurs at the interruption (I) of the coiled coil as one α-helix shifts 10 Å along the other. Other symbols: HC heavy chain; ELC essential light chain; RLC regulatory light chain; NB, nucleotide binding site. For details see text.

Steps a and b represent the binding of myosin to an actin filament and the conformational change in its head domain during ATP binding and hydrolysis. Structural studies on myosin II subfragment 1 have revealed that the actin-binding face is located on the one side of the myosin head that coincides with the central domain of the heavy-chain fragment. It is divided by a deep cleft, the apex of which merges with the pocket of the ATP binding site [14,15]. The cleft is open when the binding site is occupied by ADP together with a binding-stabilizing phosphate homologue, and closed when it is empty. Stereospecific interaction with the actin filament involves two consecutive actin monomers and

requires the cleft to be closed, which means that only the nucleotide-free molecule can bind [14,15,30,31]. The conformational change induced by the myosin-actin interaction is considered to improve the accessibility of the nucleotide binding site, specifically of its γ-phosphate position. Subsequent binding of ATP and its hydrolysis then leads to the reopening of the cleft. Data obtained by similar X-ray studies on kinesin motor domains suggest that basically the same intramolecular rearrangements are induced by nucleotide binding [16,36,37]. Notably, there is evidence that in the two-headed kinesin dimer only the one head that is bound to the microtubule, hydrolyzes ATP [38].

In myosin II the intramolecular rearrangement is associated with a change of the rod-like structure of the carboxy-terminal tail (Fig. 2c). The rod may become sharply bent at well-defined sites where the coiled-coil is weakened by skip residues [11,39]. From *in vitro* studies it has become clear that the folded rod configuration is stabilized by the binding of ADP to the active site [24]. This means that the bending must be coupled mechanically to the opening of the cleft at the actin binding site of the head. The only two ways in which the rearrangement can be communicated from the motor domain to the hinge site are a torque and a longitudinal shift of one α-helix relative to the other. Interestingly, conformational studies on myosin subfragment 1 have also shown that the α-helical domain of the myosin heavy chain involved in the formation of the coiled-coil extends straight down to the catalytic center [15,30,31].

Furthermore, nucleotide binding to the active site has been found to cause two cysteines - residues 697 and 707 in rabbit striated muscle myosin - to move towards each other by approximately 10 Å [40,41]. It must therefore be concluded that the largely α-helical segment is retracted to the same extent into the sheath formed by the NH_2-terminal region of the heavy chain and the two light chains (Fig. 2). The two heads are linked to each other at the neck region, most probably by clusters of complementary charged amino acids in the NH_2-terminal region of the heavy chains [42]. Because of the fixed positions of the heads relative to each other, the retracting α-helix moves along its inactive counterpart and exerts a bend at the hinge site of the COOH-terminal rod domain in a simple mechanical manner (Fig. 2). The important role of the head fixation in this process is supported by the finding that removal of one head leads to a loss of the bending [43]. The shift is mechanically propagated beyond the hinge site where it may induce an additional bend as observed in skeletal muscle myosin [39]. A 10Å shift corresponds closely to one α-helical heptad and therefore should not significantly affect the coiled-coil stability by itself. However, the discontinuity of the α-helical structure at the bend permits a chain rotation at the peptide bond by which a regular coiled coil can be formed up to the bend. Folded conformers are therefore more stable than the straight ones in which the presence of the skip residue leads to a more or less extended distortion of the coiled coil (Fig. 2c). The enhanced rigidity reported for folded myosin molecules [44] might result from this stabilizing effect. This stabilization entails a strong delay of $ADP{\cdot}P_i$ release from the catalytic center as the latter is

inhibited in the bent configuration [30,31]. Interestingly a similar delay of the ADP release from the catalytic center of kinesin depends in its dimeric state, suggesting that it is also due to the extensibility of the coiled-coil interaction.

The mechanochemical process

The transformation of chemical energy into kinetic energy by the various motors can be envisaged as illustrated for actomyosin in Figs. 2 and 3. During the explosive opening of the cleft induced by the ATP binding and hydrolysis, the moving head segments collide with the actin filament in a way that exerts a rotational momentum onto the motor molecule and an instantaneous disruption of the stereospecific binding. Consequently the comparatively small motor is launched at high velocity into one direction while the massive actin filament will slowly move in the opposite one (Fig. 3). Evidence for a corresponding disruptive effect caused by the opening of the cleft on the myosin-actin complex has been described [45]. Such a mechanism is further supported by the observation that inhibition of ATP hydrolysis not only suppresses the motor activity in neuronal axons but also the motor release from the vehicle [23]. Such a type of discharge must result in motor rotation typical for Brownian motion. *In vitro* evidence for such a behaviour has so far been reported for striated muscle [46,47] in which case it results from the discharge of the terminal motor molecule from the myosin filament. The momentum exerted onto the vehicle by the reaction must be equivalent to that of the expelled motor. Its direction may be parallel to the length axis as suggested by the diagram (Fig. 2a), but it is more likely to be askew to it, to an extent that depends on the spatial orientiation of the original motor-vehicle interaction. As the latter is determined by the helical path of the actin polymer, the cumulative activities of many motors propel the actin filament in its length direction. The same applies for the propulsion of microtubules owing to the helical organization of their protofilaments. This explains why none of the presently known motors move the respective vehicles askew to their length axes.

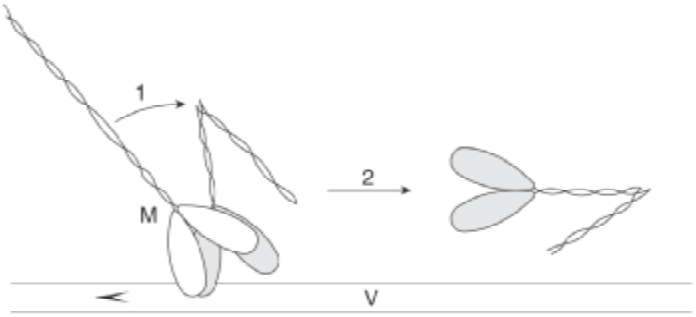

Fig. 3. Model of the mechanochemical process. The vehicle (V) is propelled (arrowhead) by the enzymatically generated rotational momentum of the motor (M). The motor molecule itself is simultaneously launched in the opposite direction as indicated by the subsequent arrows 1 and 2.

It must further be considered that a deviation of the motor stroke from the length direction imposes an angular component on the momentum of expulsion and thus causes a torsion force on the vehicle. Again, owing to the helicity of the vehicle architecture all torsional forces have the same angular direction and must thus cause the vehicle to rotate around its length axis while being propelled. Corresponding rotations of both types of vehicles during propulsion have been reported [48,49]. Studies with *in vitro* assembled microtubules have further revealed that, as predicted by the theory, the rotation-propulsion ratio depends on the steepness of the helical path of protofilaments and becomes zero if the latter is oriented parallel to the tubule axis [50].

It should be emphasized that the rotation-propulsion ratio can also become affected by the stroke-like bending exerted during the catalytic process in the rod domains of myosin II and kinesin. As the bending direction of the distal rod fragment depends on the position of the skip residues within the coiled coil, it may either weaken or strengthen the primary force of both propulsion and rotation. In fact it can even be envisaged that the momentum produced by the bending is strong enough to determine the final direction of propulsion. The latter possibility is supported by the finding that the strength of the minus-end-directed activity of ncd motor mutants can be much slower than that reached by the wild type ncd, depending on the rod-tail construct, and may even change into plus-end-directed propulsion [51].

Force-propulsion conversion

Notice that vehicle propulsion in a fluid reaches a steady state velocity when the drag exerted on the vehicle by friction equals the applied propulsion force. For jet motor-like propulsion, the drag is enhanced by the oppositely directed current, and therefore results in a correspondingly lower steady state propulsion velocity. Calculations on the conversion of propulsion force into vehicle movement depend on a variety of parameters such as the shape of vehicles and corresponding motor molecules, the geometry of flow chambers in which velocity measurements are carried out, and the position of vehicles within them.

A geometrically simple model, suitable for such a calculation is the propulsion of an actin filament in the center of a capillary of, for example, 100 µm diameter. At usual filament lengths (l) of 10 µm and a filament diameter of 10 nm, the length/width ratio is in the order of 10^3, which means that hydrodynamic effects at their ends can be neglected. First we consider the steady state fluid streaming exerted by a filament that moves with a velocity V_0 in an otherwise undisturbed fluid (Fig.4). Because of the axial symmetry of the system, the streaming velocity u(r) decreases logarithmically from the filament surface (r_f) to the capillary wall (r_c), according to

$$u(r) = u_f \cdot \ln(r/r_c)/\ln(r_f/r_c) \qquad (1)$$

where r is the distance from the axis while r_f and r_c are the radii of filament and capillary cross-sections, i.e. 0.005 µm and 50 µm respectively, u_f is the

streaming velocity at r_f and thus practically equal to V_0. To keep the filament moving at a given speed (V), a force (F) has to be applied that equals the oppositely directed friction force per unit filament propulsion, i.e.

$$F = 2 \cdot r_c \cdot \pi \cdot l \cdot \eta \cdot (u_f / d_f) / \ln (r_f / r_c) \quad (2)$$

where d_f stands for the distance moved. The corresponding velocity profile is represented by line a in Fig. 4. If the propulsion is jet-like the strokes and discharges of the motors exert a force onto a cylindrical layer at a distance r_m from the capillary center that drives the fluid in the opposite direction. The velocity profile is given by

$$F = 2 \cdot r_c \cdot \pi \cdot l \cdot \eta \cdot (u_m / d_m) / \ln (r_m / r_c) \quad (3)$$

as represented by line b in Fig. 4. Because of the equal strength of the two forces

$$u_m = u_f \cdot \ln (r_m / r_c) / \ln (r_f / r_c) \cdot d_m / d_f \quad (4)$$

The filament thus moves at a velocity V_0 in a cylindrical body of fluid that moves with a velocity of u_m in the opposite direction, thus reducing the velocity V_0 by u_m. This reduced velocity is the velocity produced by jet-like propulsion

$$V_j = V_0[1 - \ln (r_m / r_c) / \ln (r_f / r_c)] \cdot d_m / d_f \quad (5)$$

As the logarithmic factor at the given dimensions is practically equal to 1 (equ. 4), u_m can be read from Fig. 4, but because of the asymptotic relationship between V_j and r_c, the force-velocity conversion decreases with increasing capillary diameter (Fig. 4). For the same reason it increases if a vehicle is displaced from the axial position, and correspondingly, when it comes closer to the plain border in one of the usually employed flow chambers. It is for this reason that velocities of individual vehicles in a single batch vary considerably [e.g. 3,52].

The applicability of the artificial model to the actual force conversion by existing motors has to be briefly considered. Firstly, it has to be seen that the streaming generation by serial explosive motor discharges must result in local velocity fluctuations, which contrasts the steady flow pattern of the model. Such deviations from uniform flow are negligible, however, as the Reynolds' number is very low at the small dimensions of the system. Of greater importance is the fact that momentum transfer from the discharged motor to the fluid is not restricted to a given r_m but is instead partitioned over a range that extends from the vehicle surface to the most distal motor domain. An effective r_m for this experimental situation has therefore to be estimated. It changes with the size, shape and flexibility of the motor molecule, in accordance with experimental data. The propulsion velocities reached by myosin II or kinesin with truncated rod domains are lower than those reached by the respective wild type motors [53,54]. On the other hand, myosin II constructs containing a lengthened rod domain produce higher velocities than the wild type [55]. Furthermore, velocities reached with myosin I, which is smaller and more compact than myosin II, are substantially lower than those produced by the latter [56,57] and

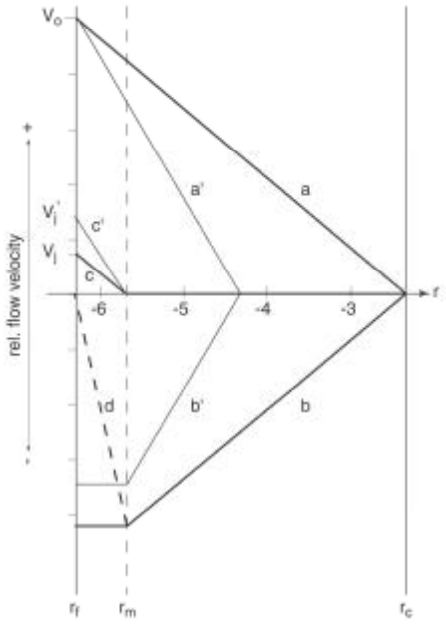

Fig. 4. Conversion of jet motor-like force generation into filament propulsion in the center of a capillary. Radial distances from the axis of the capillary to the filament surface (r_f), the site of motor activity (r_m) and the inner capillary surface (r_c) are $5 \cdot 10^{-7}$, $2 \cdot 10^{-6}$ and $5 \cdot 10^{-3}$ cm (cm logarithmic scale) respectively. V_0 is the velocity of filament movement generated by a given force in an otherwise undisturbed fluid; a is the steady-state profile of the fluid velocity produced by this movement; b is the velocity profile produced by the opposite motor force at r_m; c is the resultant flow pattern, and V_j is the filament velocity achieved by the same force by jet motor-like propulsion. a`, b`, c` and $V_j$` are the corresponding flow patterns and filament velocity at a capillary diameter of 1 μm; d (+b) is the profile of fluid flow that results if the vehicle movement is inhibited for 100% by external load. See text for further explanation.

finally, treatments that increase the myosin II flexibility by affecting the binding of the light chains to the neck region also cause a decrease of the propulsion velocity [15,44,58-60].

For myosin II bound to an actin filament the distance from the filament axis to the most distal domain is close to 25 nm, if the binding orientation is taken into account [14,15,19]. The r_m must therefore be somewhere between 5 and 25 nm. In the model we have chosen for a value of 20 nm. With this assumption the V_j calculated according to eq. 5, is only 15% of the V obtained by the same force in a stationary fluid (Fig.4). Because of the linear relation between F and u_f the jet motor-like propulsion requires a $2 \cdot 6.7$ times higher force than that required for a motor activity without an opposite plasma streaming.

Thus the energy required to keep a 10 μm long filament [l] moving at a velocity V (=u_j) is roughly $13.4 \cdot 2 \cdot r_c / \ln (r_f/r_c) \cdot l \cdot \eta \cdot u_j = 3 \cdot 10^{-17}$ kg m^2 /sec^2 or $3 \cdot 10^{-17}$ J. If the effective r_m is 5 nm more or less the required energies become $2.47 \cdot 10^{-17}$ and $3.54 \cdot 10^{-17}$ J respectively.

The distance propelled in the absence of external load depends thus on the size and shapes of motors. It further depends on the length of the filament and the velocity of its movement which contrasts with the discrete step per ATP that is predicted by the cross-bridge theory.

To understand this difference one has to realize that the force exerted onto a filament by a single motor discharge produces a propulsion that subsequently ceases exponentially by friction. If subsequent strokes occur before the velocity has decreased substantially, it adds to the actual velocity. Accordingly, the actual velocity at high stroke rates results from a number of consecutive stroke cycles, whereby the velocity increase per stroke becomes less with growing stroke rate, because of the simultaneous velocity-proportional increase of the friction. This behaviour is reflected by measurements on propulsion force obtained by Ishijima et al. [61]. They find strong force fluctuations with low force averages at low stroke rates. With increasing stroke rate, the average force increases in a saturating way. Simultaneously the force fluctuations gradually disappear. The authors point out that the cross-bridge model is incompatible with their data. They further observe that at extremely high stroke rates the force suddenly falls down to a very low level, which is also unexplainable by the cross-bridge model. A rational explanation based on the jet-like propulsion is that at high stroke rates, the velocity-proportional Reynolds'number reaches the threshold at which the laminar flow collapses. The resulting turbulence then causes inhibition of the propulsion as well disorientation of the motor activities of which only one component is measured by the employed device.

If a vehicle is kept stationary, the flow rate at r_m is almost 6.7 times the speed of free vehicle movement reached by the same motor activity (Fig.4). Obviously, such a flow can transport any particle of appropriate size with a speed conform to the local fluid velocity, a phenomenon that is generally found to be produced by motor activity along stationary vehicles *in vitro*. Such particle movements can be prevented by applying opposite forces onto them that amount up to 10 pN [62], which is likely to be equivalent to the force inherent to the local streaming. In a flow chamber that is closed on one or both ends, the streaming fluid has to be recycled at some greater distance from the filament. Such cyclic flow patterns must generally be produced by motor activities in living cells and are the only plausible cause for the well-known particle movements that deviate more or less from the direction of microtubule bundles [63].

It thus turns out that the jet propulsion-like mechanism not only fits with available data on motor structure and kinetics, but also provides rational explanations for several phenomena known from vehicle behaviour *in vitro* that are difficult to reconcile with predictions that emerge from the swinging cross-bridge theory.

CONCLUDING REMARKS AND IMPLICATIONS *in vivo*

We have shown here that a model on biological force generation can be derived from an analysis of presently available data on the structure of motor molecules and the conformational changes induced by interactions with nucleotides and by binding to microtubules or actin filaments respectively. We would like to point out that such motor activity is just a natural extension of the known mechanism of enzyme reactions facilitated by the evolution of simple structural elements in the cell. Exothermic processes are characterized by an increase of the kinetic energy of reaction partners, i.e. the enzymes and reaction products, as well as the often involved activators such as actin and tubulin dimers in the above discussed cases. As free complexes are randomly oriented, the produced kinetic energy is exclusively increasing the entropy of the system. In order to transform it into mechanically utilizable power, the complexes must be fixed into a specific spatial orientation such as is the case in the quasi-linear order of the vehicle-motor interaction. In essence, the development of motors that convert the energy derived from ATP hydrolysis into motility can be assigned to a single evolutionary step: the structural assembly of subunits that activate the ATPase, into polar linear polymers.

A crucial question is whether above calculated energy requirements match with experimental data. Measurements at roughly comparable conditions have revealed one ATP per 1 nm filament length at 5 μm propulsion [2]. For a 10 μm propulsion of a 10 μm long filament this amounts to $3 \cdot 10^{-19}$ moles ATP. The 10^{-17} J calculated above are equal to $6 \cdot 10^{-22}$ moles ATP. The much higher consumption obtained by the measurements must be ascribed to the use of filaments with lengths below 0.5 μm. Streaming along such short filaments is no more laminar and fluid turbulence causes strong friction as well as rotation of filaments around their short axes. Both effects demand large amounts of energy. Furthermore, measurements of movement encompass only the component in de focal plane and average velocities in the filament length direction become substantially higher. Taking these and other factors into account brings the two determinations into comparable ranges. There is no reason to exclude jet-like propulsion because of an unfavourable conversion of ATP hydrolysis into filament motion.

Before we can understand, how a jet motor-like force production can bring about the many phenomena for which microtubeles, actin filaments and corresponding motor activities are indispensable, we have to recognize several significant differences between the *in vitro* experiments and *in vivo* conditions. For example, the length of vehicles to which the strength of the generated force is proportional, can vary from less than 1 up to about 100 μm. The *in vivo* concentration of vehicles is usually very high, whereby the movements are reciprocally affected by each other's plasma currents, either enhancing or lowering the velocity or changing its direction. The small size of cells mostly limits the movement, and attachment of actin filaments to the cell membrane

virtually abolishes their propulsion. It is therefore not surprising that direct observation of the effects of motor activities are scarce. One clear example is the transient movement of very long microtubules into the growth cones of elongating neuronal axons, in which case it depends on the formation of bundles of microtubules with uniform polarity [7]. Another observed effect of the bundling is the plasma streaming associated with the so-called cables of actin filaments in the long characean internodial cells [6]. In agreement with the current theory the streaming direction is opposite to the *in vitro* propulsion of actin filaments. This flow amplification results from the superposition of the individual currents by a common flow pattern and therefore strengthens with increasing length and concentration of the filaments. In theory it can acquire sufficient strength to serve as a carrier for organelle transport, such as known from cytoplasmic layers and strands in highly vacuolated plant cells. Typically the transportation velocities increase with the closeness to the strands where they reach up to 50 µm per sec [64], which is ten times the velocity usually observed in *in vitro* experiments with single actin filaments. The stepping model provides no explanation for such differences.

We would like to emphasize that the generation of plasma streaming not only explains the numerous intracellular particle translocations. Rather it also helps to understand more complex cellular processes such as mitosis, cytokinesis as well as morphodynamic behaviours including muscle contraction.

Acknowledgement. We thank Prof. W. van de Water, Technical University of Eindhoven, for helpful discussions on hydrodynamic problems.

REFERENCES

1. Huxley, H.E. The mechanism of muscular contraction. **Science** 164 (1969) 1356-1365.
2. Harada, Y., Sukurada, K., Aoki, T., Thomas, D.D. and Yanagida, T. Mechanochemical coupling in actomyosin energy transduction studies by *in vitro* movement assay. **J. Mol. Biol.** 216 (1990) 49-68.
3. Paschal, B.M., Shpetner, H.S. and Vallee, R.B. MAP 1C is a microtubule-activated ATPase which translocates microtubules *in vitro* and has dynein-like properties. **J. Cell Biol.** 105 (1987) 1273-1282.
4. Paschal, B.M. and Vallee, R.B. Retrograde transport by microtubule-associated protein MAP 1C. **Nature** 330 (1987) 181-183.
5. Pollack, G.H. The cross-bridge theory. **Physiol. Rev.** 63 (1983) 1049-1113.
6. Kersey, Y., Hepler, P.H., Palewitz, B.A. and Wessels, N.K. Polarity of actin filaments in Characean algae. **Proc. Natl. Acad. Sci. U.S.A.** 73 (1976) 165-167.
7. Tanaka, E.M. and Kirschner, M.W. Microtubule behaviour in the growth cones of living neurons during axon elongation. **J. Cell Biol.** 115 (1991) 345-363.

8. Vale, R.D., Reese, T.S. and Sheetz, P.M. Identification of a novel force-generating protein, kinesin, involved in microtubule based motility. **Cell** 42 (1985) 39-50.
9. Kron, S.J. and Spudich, J.A. Fluorescent actin filaments move on myosin fixed to a glass surface. **Proc. Natl. Acad. Sci. U.S.A.** 83 (1986) 6272-6276.
10. Toyoshima, Y.Y., Kron, S.J., Mcnally, E.M., Niebling, K.R.N., Toyoshima, C. and Spudich, J.A. Myosin subfragment-1 is sufficient to move actin filaments *in vitro*. **Nature** 328 (1987) 536-539.
11. Yang, J.T., Laymon, R.A. and Goldstein. L.S. B. A three-domain structure of kinesin heavy chain, revealed by DNA sequence and microtubule binding analysis. **Cell** 56 (1989) 879-889.
12. Kuznetsov, S.A., Vaisberg, E.A., Shanina, N.A., Magretova, N.N., Chernak, V.Y. and Gelfand, V.I. The quaternary structure of bovine kinesin. **EMBO-J.** 7 (1988) 353-356.
13. Kuznetsov, S.A., Vaisberg, E.A., Rothwell, S.W., Murphy, D.B. and Gelfand, V.I. Isolation of a 45-kDa fragment from kinesin heavy chain with enhanced ATPase and microtubule binding activities. **J. Biol. Chem.** 264 (1989) 589-595.
14. Rayment, I., Holden, H.M., Whittaker, M., Yohn, C.B., Lorenz, M., Holmes, K.C. and Milligan, A.R. Structure of the atin-myosin complex and its implications for muscle contraction, **Science** 261 (1993) 58-65.
15. Rayment, I., Rypniewski, W.R., Schmidt-Bläse, K., Smith, R., Tomchik, D. R., Benning, M.M., Winkelmann, D.A., Wesenberg, G. and Holden, H.M. Three-dimensional structure of myosin subfragment-1: a molecular motor. **Science** 261 (1993) 50-58.
16. Kull, F.J., Sablin, E.P., Lace, R., Fletterich, R.J. and Vale R.D. Crystal structure of the kinesin motor domain reveals a structural similarity to myosin. **Nature** 380 (1996) 550-555.
17. Conzelman, K.A. and Mooseker, M.S. The 110-kD protein-calmodulin complex of the intestinal microvillus is an activated MgATPase**. J. Cell Biol.** 105 (1987) 13-324.
18. Song, Y. -H. and Mandelkow, E. Recombinant kinesin motor domain binds to β-tubulin and decorates microtubules with a B surface lattice. **Proc. Natl. Acad. Sci. U.S.A.** 90 (1993) 1671-1675.
19. Huxley, H.E. Electron microscope studies of the structure of natural and synthetic protein filaments from striated muscle. **J. Mol. Biol.** 7 (1963) 281-308.
20. Porter, M.E., Scholey, J.M., Stemple, D.L., Vigers, G.P.A., Vale, R.D. Sheetz, M.P. and Mcintosh, J.R. Characterization of the microtubule movement produced by sea urchin egg kinesin. **J. Biol. Chem.** 262 (1987) 2794-2802.
21. Clarke, M. and Spudich, J.A. Biochemical and structural studies of actomyosin-like proteins from amoebae of Dictyostelium discoideum. **J. Mol. Biol.** 86 (1974) 209-222.

22. Kuznetsov, S.A. and Gelfand, V.I. Bovine brain kinesin is a microtubule-activated ATPase. **Proc. Natl. Acad. Sci. U.S.A.** 83 (1986) 8530-8534.
23. Pfister, K.K., Wagner, M.C., Bloom, G.S. and Brady, S.T. Modification of the microtubule-binding and ATPase activities of kinesin by N-ethylmaleimide [NEM] suggests a role for sulfhydryls in fast axonal transport. **Biochemistry** 28 (1989) 9006-9012.
24. Cross, R.A., Cross, K.K. and Sobiszek, A. ATP-linked monomer-polymer equilibrium of smooth muscle myosin: the free folded monomer trap ADP· P_i. **EMBO-J.** 5 (1986) 2637-2641.
25. Hackney, D.D. Kinesin ATPase: rate-limiting ADP release. **Proc. Natl. Acad. Sci. U.S.A.** 85 (1988) 6314-6318.
26. Gilbert, S.P. and Johnson, K.A. Pre-steady-state kinetics of the microtubule-kinesin ATPase**. Biochemistry** 33 (1994)1951-1960.
27. Lockhart, A. and Cross, A.R. Origins of reversed directionality in the ncd molecular motor. **EMBO-J.** 13 (1994) 751-757.
28. Gibbons, I.R., Cosson, M.P., Evans, J.A., Gibbons, B.H., Houk, B., Martinson, K.M., Sale, W.S. and Tang, W.-J.Y. Potent inhibition of dynein adenosinetriphosphatase and motility of cilia and sperm flagella by vanadate **Proc. Natl. Acad. Sci. U.S.A.** 75 (1978) 2220-2224.
29. Beckerle, M. and Porter K.R. Analysis of the role of microtubules and actin in erythrophore intracellular motility. **J. Cell Biol.** 96 (1983) 354-362.
30. Fisher, A.J., Smith, C.A., Thoden, J., Smith, R., Sutoh, K., Holden, H.M. and Rayment, J. Structural studies of myosin:nucleotide complexes: a revised model for the molecular basis of muscle contraction. **Biophys. J.** 68 (1995) 19S-28S.
31. Fisher, A.J., Smith, C.A., Thoden, J.B., Smith, R., Sutoh, K., Holden, H.M. and Rayment, I. X-ray structures of myosin motor domain of Dictyostelium discoideum complexed with MgADP·BeF_x and MgADP· AlF4. **Biochemistry** 34 (1995) 8960-8972.
32. Crevel, I.M., Lockhart, A. and Cross, R.A. Weak and strong states of kinesin and ncd. **J. Mol. Biol.** 257 (1996) 66-76.
33. Omoto, C.K. and Johnson, K.A. Activation of the dynein adenosinetriphosphatase by microtubules. **Biochemistry** 25 (1986) 419-427.
34. Shimizu, T., Marchese-Ragona, S.P. and Johnson, K.A. Activation of dynein adenine triphosphatase by cross-linking to microtubules. **Biochemistry** 28 (1989) 7016-7021.
35. Shimizu, T., Toyoshima, Y. ., Edamatsu, M. and Vale, R.D. Comparison of the motile and enzymatic properties of two microtubule minus-end-directed motors, ncd and cytoplasmic dynein. **Biochemistry** 43 (1995) 1575-1582.
36. Sablin, E.P., Kull, F.J., Cooke, R., Vale, R.D. and Fletterich, R.J. Crystal structure of the motor domain of the kinesin-related motor ncd. **Nature** 380 (1996) 555-559.
37. Kull. F.J. and Endow, S.A. Kinesin: swich I & II and the motor mechanism. **J. Cell Sci.** 115 (2002) 15-23.

38. Hackney, D.D. Evidence for alternating head catalysis by kinesin during microtubule-stimulated ATP hydrolysis**. Proc. Natl. Acad. Sci. U.S.A**. 91 (1994) 6865-6869.
39. Offer, G. Skip residues correlate with bends in the myosin tail. **J. Mol. Biol.** 216 (1990) 213-218.
40. Burke, M. and Reisler, E. Effect of nucleotide binding on the proximity of the essential sulfhydryl groups of myosin. Chemical probing of movement of residues during conformational transitions. **Biochemistry** 16 (1977) 5559-5563.
41. Huston, E.E., Grammer, J.C. and Yount, R.G. Flexibility of the myosin heavy chain: direct evidence that the region containing SH_1 and SH_2 can move 10Å under the influence of nucleotide binding. **Biochemistry** 72 (1988) 8945-8952.
42. Onishi, H., Maita, T., Matsuka, G. and Fujiwara, K. Lys-65 and Glu-168 are the residues for carbodiimide-catalysed cross-linking between the two heads of rigor smooth muscle heavy meromyosin. **J. Biol. Chem.** 265 (1990) 19362-19368.
43. Olney, J.J., Sellers, J.R. and Cremo, C.R. Structure and function of the 10S conformation of smooth muscle myosin. **J. Biol. Chem.** 217 (1996) 20375-20384.
44. Rosenfeld, S.S., Xing, J., Rener, B., Lebowitz, J., Karr, S. and Cheung, H.C. Structural and kinetic studies of the 10S↔6S transition in smooth muscle myosin. **J. Biol. Chem.** 269 (1994) 30187-30194.
45. Mendelson, R. and Morris, E.P. The structure of the acto-myosin subfragment 1 complex: Results of searches using data from electron microscopy and X-ray crystallography. **Proc. Natl. Acad. Sci.** 94 (1997) 8533-8538.
46. Reedy, M.K., Lucaveche, C., Naber, N. and Cooke, R. Insect cross-bridges, relaxed by spin-labeled nucleotide, show well-ordered 90º state by X-Ray diffraction and electron microscopy but spectra of electron paramagnetic resonance probes report disorder. **J. Mol. Biol.** 227 (1992) 678-697.
47. Zhao, L., Naber, N. and Cooke, R. Muscle cross-bridges bound to actin are disordered in the presence of 2,3-butanedione monoxime. **Biochem. J.** 68 (1995) 1980-1990.
48. Nishizaka, T., Yagi, T., Tanaka, Y. and Ishiwata, S. Right handed rotation of an actin filament in an *in vitro* motile system. **Nature** 361 (1993) 269-271.
49. Sase, I., Miyata, H., Ishiwata, S. and Kinosita, K. jr. Axial rotation of sliding actin filaments revealed by single-fluorophore imaging. **Proc. Natl. Acad. Sci. U.S.A.** 94 (1997) 5646-5650.
50. Ray, S., Meyhover, E., Milligan, R.A. and Howard, J. Kinesin follows the microtubule's protofilament axes. **J. Cell Biol.** 121 (1993) 1083-1093.
51. Henningsen, U. and Schliwa, M. Reversion in the direction of movement of a molecular motor. **Nature** 389 (1997) 93-96.

52. Harada, Y., Noguchi, A., Kishino, A. and Yanagida, T. Sliding movement of single actin filaments on one-headed myosin filaments. **Nature** 326 (1987) 805-808.
53. Waller, G.S., Ouyang, G., Swafford, J., Vibert, P. and Lowey, S. A minimal motor domain from chicken skeletal muscle myosin. **J. Biol. Chem.** 270 (1995) 15348-15352.
54. Stewart, R.J., Thaler, J.P. and Goldstein, L.S.B. Direction of microtubule movement is an itrinsic property of the motor domains of kinesin heavy chain and Drosophila ncd protein. **Proc. Natl. Acad. Sci. U.S.A.** 90 (1993) 5209-5213.
55. Ansow, M. Geeves, M.A. Kurozava, S.E. and Manstein, D.J. Myosin motors with artificial lever arms. **EMBO-J.** 15 (1996) 6069-6074.
56. Wolenski, J.S., Hayden, M.S., Forscher, P. and Mooseker, M.S. Calcium-calmodulin and regulation of brush border myosin-I MgATPase and mechanochemistry. **J. Cell Biol.** 122 (1993) 613-621.
57. Cheney, R.E., O'Shea, M., Heuser J.E., Coelho, M.V., Wolenski, J.S. Espreatico, E.M. Forscher, F., Larson, R.E. and Mooseker, M.S. Brain myosin-V is a two-headed unconventional myosin with motor activity. **Cell** 75 (1993) 13-23.
58. Lowey, S., Waller, G.S. and Trybus, K.M. Skeletal muscle myosin light chains are essential for physiological speeds of shortening. **Nature** 365 (1993) 454-456.
59. Van Buren, P., Waller, G.S., Harris, D.E., Trybus, K.M., Warshaw, D.M. and Lowey, S. The essential light chain is required for full force production by skeletal muscle myosin. **Proc. Natl. Acad. Sci. U.S.A.** 91 (1994) 12403-12407.
60. Xie, X., Harrison, D.H., Schlichting, I., Sweet, R.-M., Kalabokis, V.N., Szent-Györgyi, A.G. and Cohen, C. Structure and regulatory domain of scallop myosin at 28Å resolution. **Nature** 368 (1994) 306-312.
61. Ishijima, A., Doi, T., Sakurada, K. and Yanagida, T. Sub-piconewton force fluctuations of actomyosin *in vitro*. **Nature** 352 (1991) 301-306.
62. Visscher, K., Schnitzer, M.J. and Black, S.-M. Single kinesin molecules studied with a molecular force clamp. **Nature** 400 (1999) 184-189.
63. Bajer, A. and Molé-Bajer, J. Spindle dynamics and chromosome movement. **Int. Rev. Cytol.** 3 (1972) Supl. 3, 1-217.
64. Williamson, R.E. Cytoplasmic streaming in Chara: A cell model activated by ATP and inhibited by cytochalasin. **J. Cell Sci.** 17 (1975) 655-668.